NON-LINEAR COMPANDING TECHNIQUES WITH ACO-OFDM-BASED VLC SYSTEMS FOR PAPR REDUCTION

Ashraf A. M. Khalaf[1], Mohamed M. Elnabawy[2], *, Nazmi A. Mohammed[3]

[1]*Dept. of Electronics & Communications Engineering, Faculty of Engineering, Minia University, Minia 61111, Egypt.*

[2]*Electronics and communication Department, Modern Academy for Eng & Tech, Maadi 11585, Cairo, Egypt.*

[3]*Photonic Research Lab, Electrical Engineering Department, College of Engineering, Dawadmi, Shaqra University, Kingdom of Saudi Arabia, 11961. OSA Member.*

Corresponding Author E-mail: eng.mohamed.elnabawy@gmail.com

ABSTRACT

In visible light communication (VLC) systems, optical orthogonal frequency division multiplexing (OOFDM) is used to reduce the effects of inter-symbol interference while simultaneously achieving fast data transmission speeds and large bandwidths. Asymmetrically clipped optical orthogonal frequency division multiplexing (ACO-OFDM) is one of the most OOFDM used. ACO-OFDM with low peak-to-average power ratio performance becomes essential for practical visible light communication broadcasting systems due to non-linearity elimination. The techniques for reducing the peak-to-average power ratio for visible light communication broadcasting systems are designed, simulated, and evaluated in this work. This work provides novel mixed Non-Liner Companding Techniques that target remarkable peak-to-average power ratio performance with acceptable bit error rate performance for ACO-OFDM-based VLC systems. This work compares the designed techniques then nominates an optimum one that provides the optimum peak-to-average power ratio and bit error rate performance. Finally, the nominated technique will be compared to all related literatuers of ACO-OFDM-based VLC systems to ensure its novelty, validity, and effectiveness.

1. INTRODUCTION

In visible light communication (VLC), data is transmitted using light-emitting diodes (LEDs) in the visible light spectrum. VLC is a highly efficient wireless data transmission method in indoor environments, particularly for low mobility and short-range [1]. Compared to radiofrequency (RF) systems, these systems have various advantages, including lower implementation costs, free licensing bandwidth, a unique feature of VLC technology, enhanced privacy, and security because light rays cannot pass through barriers [2].

Furthermore, VLC has advanced to the level of state-of-the-art optical communication technology. It is an advanced version of free-space optical communication (FSO) [3], particularly useful for indoor applications. Numerous optoelectronic/photonic devices/platforms, including fiber Bragg gratings (FBGs) [4–6], Mach Zehnder interferometers (MZIs) [7,8], and semiconductor optical amplifiers (SOAs), began to focus and switch some of their applications in response to the noticeable spread of VLC technology, particularly in indoor optical communication environments. Recently, photonic crystal (PhC) technologies and platforms have been recommended for integration with VLC system components due to their promising power and efficiency

characteristics [9–12].

Several applications, including localization, high-speed video streaming, high bit-rate data broadcasting in indoor buildings, and underwater data transmission, make use of VLC. It is also preferred in high- electromagnetic interference (EMI) environments, such as aircraft and vehicle-to-vehicle communication systems [2,13,14]. VLC and dense wavelength division multiplexing are incorporated into emerging communication technologies, such as the 5G mobile communication system [4]. In indoor buildings, VLC data broadcasting is a fast emerging topic of research that readily meets lighting and connectivity requirements [15]. Different modulation techniques are used to achieve dimming control (i.e., controlling illumination levels) while maintaining communication linkages. Techniques for VLC modulation are broadly categorized into two categories: single carrier modulation (SCM) and multicarrier modulation (MCM). It is worth noting that SCM techniques like pulse amplitude modulation (PAM), pulse position modulation (PPM), pulse width modulation (PWM), and on-off keying (OOK) are utilized to construct a VLC system at low operating system rates. However, at higher operating bit rates, SCM approaches are imposed on the problem of inter-symbol interference (ISI) [16,17]. MCM techniques are introduced, with optical orthogonal frequency division multiplexing (OOFDM) as the nominated methodology, to alleviate the shortcomings of SCM techniques. MCM approaches are discussed as possible modulation techniques for high-speed VLC communication systems and applications in the future. Regrettably, this compromises the system's complexity [3,18–20].

OOFDM is a modulation method that is considered to be attractive for extending the modulation bandwidth of LEDs [19]. Numerous OOFDM methods have been proposed recently. Asymmetrically clipped optical OFDM (ACO-OFDM) [21], flip OFDM, and unipolar OFDM (U-OFDM) [22] all have the potential to achieve higher power efficiency than conventional direct-current biased optical orthogonal frequency division multiplexing (DCO-OFDM) at the cost of a half-division of spectral efficiency [23]. To compensate for the loss of spectral performance, enhanced unipolar OFDM (eU-OFDM) [24], spectral and energy-efficient OFDM (SEE-OFDM) [25], and polar OFDM (P-OFDM) are added. Fundamentally, eU-OFDM and SEE-OFDM are identical. These concepts are demonstrated by combining multiple signals at the transmitter and demodulating them independently at the receiver. However, increasing the number of signal pathways and system complexity improves spectral efficiency. In P-OFDM, a polar coordinate transformation is employed to generate the proper signal structure for VLC transmission without imposing a cost on spectral efficiency. To summarise, ACO-OFDM is a critical scheme based on many previously optimized schemes with enhanced features. The last concept, together with the previously described advantages of ACO-OFDM and the fact that it is one of the most feasible schemes for VLC communication systems in use today, motivates this work to focus on this type in particular [26–28].

All MCM approaches experience significant difficulties when used for high-speed VLC communication. The Peak-to-Average Power Ratio (PAPR) and the complexity of producing and demodulating MCM signals are two issues that must be addressed. According to [23], the fundamental disadvantage of MCM techniques is that they generate transient peaks over the OFDM signal, contributing significantly to PAPR. The presence of PAPR is most noticeable during the creation of the OFDM/OOFDM signal from parallel data streams. When the subcarrier-modulated symbols are applied in the same step as the carrier-modulated symbols, the signal reaches its maximum power. OFDM has several inherent disadvantages because of the high PAPR values, including non-linear signal distortions and high demand for transmitter amplifier

power [29,30].

The following illustrates the problem's inception in VLC: LEDs are utilized as transmitters, and high-power transmissions can cause them to malfunction. LEDs have a small operating voltage range, and the voltage-to-current (V-I) relationship is non-linear in comparison to other types of lighting. The non-linear V-I characteristic of LEDs distorts the OFDM signal when the PAPR is high. Because of their high peak power, LED chips are susceptible to overheating. Consequently, the high PAPR of the OFDM signal should be reduced until it is fed into the transmitter LEDs before it is sent [31,32].

Based on the strategy, PAPR reduction approaches for MCM techniques can be split into three types: coding techniques (CT)/precoding techniques (PCT), multiple signal representation (MSR) techniques, and adding signal techniques (AST) [33]. CT can increase computational complexity, side information, or the number of subcarriers used, all of which are inefficient for high-speed VLC-OOFDM communication. The disadvantages of CT can be minimized with the use of PCT [28]. Using MSR techniques, alternate signals for the same signal are generated by modifying the original signal's phases, amplitude, and phases or data locations. The key disadvantages of this strategy include increased computational complexity and the requirement to broadcast side information for the receiver, which affects the efficiency of the available bandwidth. The Partial Transmit Sequence (PTS) and Selective Mapping (SLM) techniques are the two most common types of MSR [34–36].

Finally, AST reduces the PAPR in three ways: signal clipping, compressing large peaks using the non-linear compression transform (NCT) and applying peak reduction signal/or stretch the constellation. These techniques generate undesired distortion noise into the broadcast stream. NCT is a highly effective and extensively utilized technology [37–39]. In NCT, the companding function is applied to the initial OOFDM signal to increase the amplitude of small signals and compress the amplitude of large signals. The companding function can be used to maintain the signal's average power constant. The most common types of NCT include exponential, A-law, μ -law, and rooting compensating techniques (RCT) [40–43].

The work's originality is based on two key aspects. First, to the author's best knowledge, it is the first time exploring the effect of applying types of rooting companding techniques (RCT) on the PAPR and BER performance in a VLC based system be discussed in section 4.1. Second, to the author's best knowledge, BER and PAPR performance will be explored using A-law companding techniques combined with RCT (A-RCT) and μ-law companding technique combined with RCT (μ-RCT). The combined analysis will be carried out in section 4.2. Section 4.3 will present a comparison of all of these strategies' PAPR and BER performance.

The following is the structure of the paper: Section 2 discusses the ACO-OFDM System model and the PAPR system. Section 3 discusses PAPR Reduction strategies as well as the planned PAPR Reduction system in further detail. Section 4 discusses the simulation results and compares the proposed approaches. An evaluation of both the current study and the existing literature reviews is discussed in section 5. Section 6 presents the conclusion.

2. Model of the ACO-OFDM System and PAPR

In Fig. 1, a normal IM/DD optical wireless transmission scheme with ACO-OFDM and N subcarriers. When using quadrature-amplitude modulation (QAM), the transmitted bit stream is converted to complex-valued symbols, A_k $k = 0,1,\cdots,N-1$. Time-domain signals are real-valued because OFDM subcarriers are Hermitian symmetric, which means that $A_k = A^*_{N-k}$, $k = 1,2,\dots,N/2 - 1$. To ensure that the time-domain signals can be explicitly clipped at zero, only odd subcarriers are modulated. The

frequency-domain ACO-OFDM signals are denoted by [44],

$$A = [0, A_1, 0, A_3, \ldots, A_{N/2-1}, 0, A^*_{N/2-1}, \ldots, A^*_1],$$ (1)

The time-domain ACO-OFDM signal is obtained using the Inverse Fast Fourier Transform (IFFT) as follows:

$$a_{ACO,n} = \frac{1}{\sqrt{N}} \sum_{k=0}^{N-1} A_k \exp\left(j \frac{2\pi}{N} kn\right),$$ (2)

$$n = 0,1, \cdots, N-1,$$

Which follows a half-wave symmetry as:

$$= -a_{ACO,n+N/2},$$

$$n = 0,1, \cdots, N/2 - 1.$$ (3)

As a result, the negative component of the signal can be eliminated without sacrificing any information:

$$[a_{ACO,n}]_c = a_{ACO,n} + i_{ACO,n}$$

$$= \begin{cases} a_{ACO,n}, & a_{ACO,n} \geq 0; \\ 0, & a_{ACO,n} \leq 0; \end{cases}$$ (٤)

For $n = 0,1, \cdots, N-1$, where $i_{ACO,n}$ shows the ACO-OFDM negative clipping distortion signal.

Even after the IFFT procedure, the beginning of each time-domain OFDM symbol is prefixed with a cyclic prefix (CP) to eliminate ISI at the receiver. After converting the signal from parallel to serial (P/S), it is clipped at zero and modulated by the LEDs [26].

A photodiode (PD) detects the optical signal and transforms it into an electrical signal at the receiver. According to [45], At the receiver, a PD detects the optical signal and transforms it into an electrical signal. According to [45], when translated to the frequency domain, negative clipping distortion occurs exclusively on even subcarriers, and it is orthogonal to the transmitted data on odd subcarriers. Thus, employing an essential FFT operation at the receiver, the transmitted signal of the odd subcarriers can be retrieved after serial-to-parallel (S/P) conversion and CP exclusion.

The PAPR statistic for an OOFDM signal is the ratio of the maximum power to the average power, which is [46]:

$$PAPR = \frac{max\left\{\left|[a_{ACO,n}]_c\right|^2\right\}}{E\left|[a_{ACO,n}]_c\right|^2}$$ (5)

Where E{.} stands for the statistical expectation.

When evaluating the output of the PAPR reduction technique, it is common to employ the complementary cumulative distribution function (CCDF) to provide it. The CCDF is the probability that an OOFDMsignal's PAPR is greater than the given threshold PAPR ($PAPR_0$), expressed as:

$$= P(PAPR > PAPR_0)$$
$$= 1 - (1 - e^{-PAPR_0})^N$$ (6)
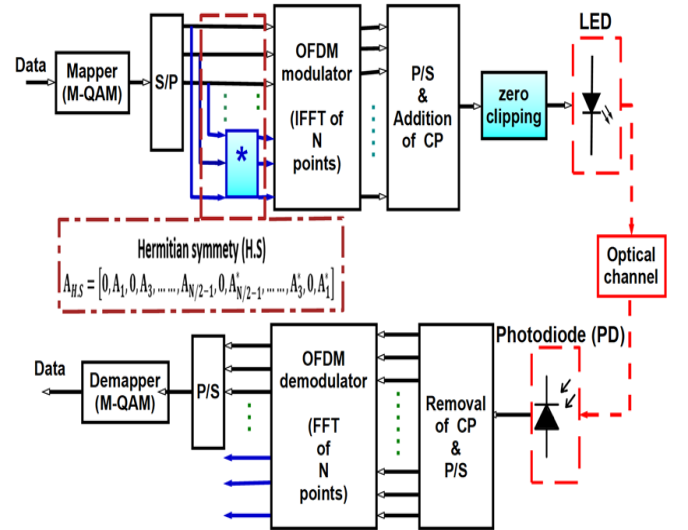
Fig. 1. Conventional ACO-OFDM-based VLC system.

3. PAPR REDUCTION TECHNIQUES AND PROPOSED MODEL

This section is comprised of two major sections. Section 3.1 discusses the mathematical modeling of NCT and its inverse. Section 3.2 discusses the proposed VLC system that utilizes NCT for ACO-OFDM.

3.1. Non-linear Companding Techniques (NCT)

Non-linear companding schemes are

among the most appealing techniques used to reduce PAPR in the MCM system due to its better performance, BER, lack of bandwidth, and soft implementation complexity. The non-linear companding scheme performs compression at the transmitter end and expansion at the receiver side before the signal enters to analysis filter. It uses precisely monotonically increasing companding function. Therefore, the output companded signal at the transmitter side can easily recover at the receiver side using the inverse companding function. The SQRT companding, A-law, μ-Law, and RCT companding techniques are types of non-linear companding.

3.1.1. μ-law companding transform

In μ-law companding, the compressor characteristic is piecewise, having a linear segment for low-level inputs and a logarithmic segment for high-level inputs. The signal is compressed and expanded at the transmitter and receiver, respectively. [47] has the compressing:

$$A_c(n) =$$
$$V_{max} \frac{\log\left(1 + \mu\left|\overline{A}(n)\right|/V_{max}\right)}{\log(1 + \mu)} \text{sgn}\left[\overline{A}(n)\right]^{(\vee)}$$

Where$V_{max} = max\left(\overline{A}(n)\right)$ $n = 0,1,\dots,N-1$. μ is a companding parameter that is adjustable and can be used to modify the amount of PAPR reduction for OFDM signals. The sample has been blended with $A_c(n)$. $\overline{A}(n)$ is the sample's source.

The method of expansion is essentially the inverse of the method of expansion in Equation 7. as shown below:

$$\hat{\overline{A}}(n) =$$
$$\frac{V_{max}}{\mu}\left[exp\left[\frac{|A_c(n)|ln[1+\mu]}{V_{max}}\right]\right]\text{sgn}[A_c(n)] \quad 8)$$

The sample that was calculated after the expansion is denoted by $\hat{\overline{A}}(n)$.

3.1.2. A-law companding transform

In this companding form, the compressor characteristic is represented piecewise as a function of input level, with a linear segment for low-level inputs and a logarithmic section for high-level inputs. [48] The PAPR, which is the fundamental disadvantage of OFDM, can be reduced by using this method.

$$y(x) = \begin{cases} y_{max}\dfrac{A\dfrac{|x|}{x_{max}}}{(1+A)}sgn(x), & 0 < \dfrac{|x|}{x_{max}} \leq \dfrac{1}{A} \\[6mm] y_{max}\dfrac{\left[1 + \log_e\left[A\dfrac{|x|}{x_{max}}\right]\right]}{(1+\log_e A)}sgn(x), & \dfrac{1}{A} < \dfrac{|x|}{x_{max}} \leq 1 \end{cases} \quad (٩)$$

Where x: input signal, y: output signal, and A is a companding factor.

3.1.3. Rooting companding transform (RCT)

Rooting companding Transform (RCT) has been inspired by the square root transform principle (SQRT). The RCT process is applied to all OFDM output symbols; therefore, the PAPR is reduced without sending side information. The RCT process changes the distribution of the power signals to Rayleigh distribution and reduces the value of average power from N to $N^{1/R}$. Rooting companding function is described by

$$A_c(n) = \overline{A}(n)^R * \text{sgn}\left[\overline{A}(n)\right], \quad (10)$$
$$0.1 \leq R \leq 0.9$$

Where $A_c(n)$ is the sample that has been combined. $\overline{A}(n)$ is the original sample. The amount of companding depends on R. when R=0.5, the type of companding technique is SQRT.

The rooting decompanding function is described by

$$\hat{\overline{A}}(n) = A_c(n)^{\frac{1}{R}} * \text{sgn}\left[A_c(n)\right] \quad (١١)$$

3.2. sed PAPR reduction systemoporP

The proposed companding approaches for the ACO-OFDM-based VLC system are depicted in Figure 2. It is distinguished from

the traditional one (i.e., Fig. 1) by the figure's proposed units represented in green. 2. Section 3.1 discusses the mathematical description and guidelines for proposed units.

Following the first section's novelty points, examining the impact of NCT types on PAPR and BER performance in a VLC-based system will use green units. This will be carried out in section 4—as previously mentioned. Section 4.1 describes the performance of both BER and PAPR using RCT only. The A-law combined with RCT (A-RCT) will be presented in section 4.2. Section 4.3 describes the performance of both BER and PAPR using μ-law combined with RCT (μ-RCT). A comparison between the RCT, A-RCT, and μ-RCT will be presented in section 4.4.
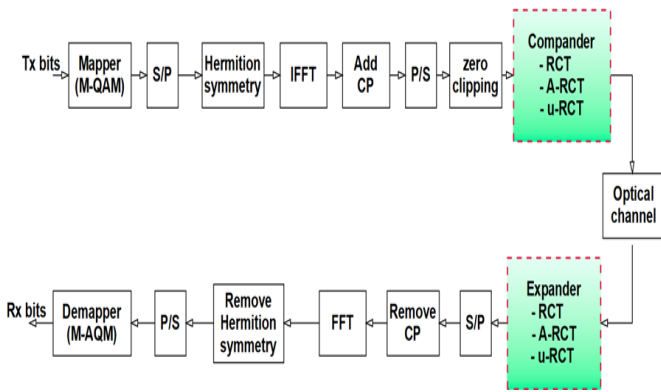
Fig. 2. Proposed companding techniques for ACO-OFDM-based VLC system

4. SIMULATION RESULTS

The following sections will use the parameters listed below from the available literature (i.e., RF and VLC). Order of modulation utilizing 16-QAM symbols. For the number of subcarriers, M = 256 and N = 1024 IFFT points are assumed. Its CCDF determines the effectiveness of the PAPR reduction. The values of $PAPR_0$ is calculated at $CCDF=10^{-3}$ to be 17 dB for conventional ACO-OFDM.

The PAPR reduction value (i.e., which will be presented in detail in section 4.3 Table 1) is calculated as the difference between the conventional ACO-OFDM

$PAPR_0$ (i.e., 17dB) and the $PAPR_0$ for the technique under evaluation is a critical evaluating parameter for this technique. The greater the PAPR reduction value, the more effective the technique used. This is the primary objective of this work.

Another criterion for evaluation is $E_b/N_{0\ diff}$. it is the difference between E_b/N_0 for the technique under evaluation and the E_b/N_0 for conventional ACO-OFDM (i.e. 13.5dB) at $BER=10^{-3}$. The factor of $E_b/N_{0\ diff}$ estimates whether the tested technique needs more/or less power to achieve the target BER (i.e., $=10^{-3}$) compared to conventional ACO-OFDM. The higher the $E_b/N_{0\ diff}$ with values greater than zero, this means that we need more power to achieve the targeted BER (i.e., $=10^{-3}$) compared to the conventional ACO-OFDM and hence lousy performance. This performance benefit, however, is obtained at the expense of the value being set below zero. The following sections (in particular, section 4.3) will be focused on this basic idea: evaluating BER performance (Table 1).

4.1.Exploring PAPR and BER for RCT

As indicated previously, this section evaluates PAPR and BER performance when applying RCT on ACO-OFDM Based VLC systems with the aforementioned parameters.

Figure. 3 explores PAPR performance when applying RCT to the proposed VLC system (i.e., Fig. 2). The companding value of RCT is controlled by the Rooting factor (RF). The figure also contains the performance of conventional ACO-OFDM (i.e., Fig. 1) for comparison purposes. In the RCT companding technique, the rooting factor (RF) varies from 0.1 to 0.9 by step size 0.1. At $CCDF=10^{-3}$, when RF 0.1, 0.2, 0.3, 0.4, 0.5, 0.6, 0.7, 0,8 and 0.9, the value of $PAPR_0$ equals 4.9, 6.6, 8.1, 9.7, 10.9, 12.4, 13.4, 14.3, and 15.7, respectively. This means that the RCT technique causes the reduction of the PAPR parameter compared to conventional ACO-OFDM by decreasing the value of RF. The reduction value for the different RF-parameters values equals 12.1, 10.4, 8.9, 7.3, 6.1, 4.6, 3.6, 2.7, and 1.3, respectively.
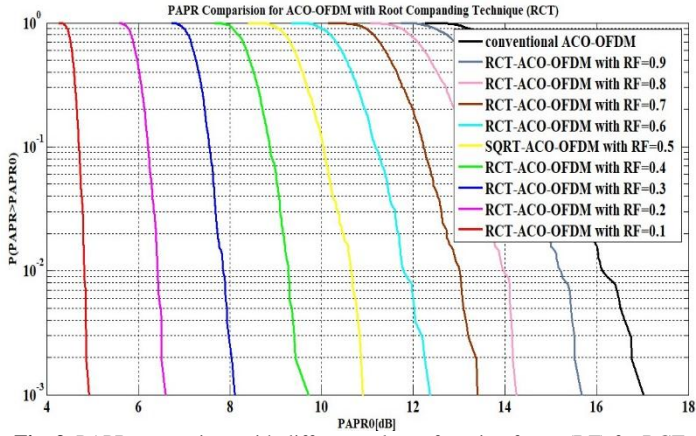
Fig. 3. PAPR comparison with different values of rooting factor (RF) for RCT-ACO-OFDM-based VLC system.

Figure. 4 explores BER performance when applying RCT to the proposed VLC system (i.e., Fig. 2). The figure also contains the performance of conventional ACO-OFDM (i.e., Fig. 1) for comparison purposes. At BER=10^{-3}, the value of E_b/N_0 for conventional ACO-OFDM equals 13.5dB. When applying RCT techniques, BER is improved for companding factor RF equals 0.6, 0.7, 0.8, and 0.9. For RF equals 0.6, 0.7, 0.8, and 0.9, the required E_b/N_0 to achieve BER=10^{-3} are 13.2, 12.5, 12.3, and 12.7dB, respectively. This means that saving power occurs (better BER performance) by 0.3, 1, 1.2, and 0.8dB, respectively, to achieve a target BER compared to conventional ACO-OFDM. For RF equals 0.5, 0.4, 0.3, 0.2 and 0.1, the required E_b/N_0 to achieve BER=10^{-3} are 14.6, 16.5, 19.3, 23.2, and 29.8dB, respectively. Thus, increased values in E_b/N_0 compared to conventional ACO-OFDM by 1.1, 3, 5.8, 9.7, and 16.3 dB.
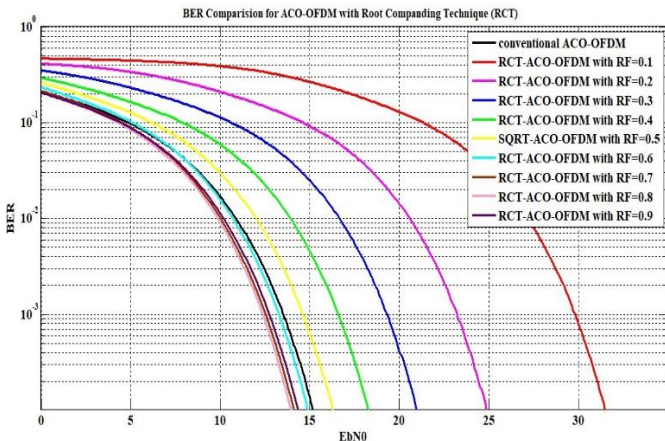
Fig. 4. BER comparison with different values of rooting factor (RF) for RCT-ACO-OFDM-based VLC system.

At the high RF (i.e., from 0.6 to 0.9), RCT companding techniques show an attractive performance by reducing PAPR while improving BER performance. At RF=0.5, the RCT techniques are called square rooting techniques (SQRT). The SQRT is attractive PAPR reduction value, while the Penalty of BER performance is in suitable value.

4.2. Exploring PAPR and BER for A-RCT and µ-RCT.

As previously stated, this section evaluates the PAPR and BER performance when A-law and µ-law companding techniques are used in combination with RCT on ACO-OFDM-based VLC systems using the aforementioned parameters. At combined A-law with RCT, the proposed system is called the A-RCT-ACO-OFDM system. At combined µ-law with RCT, the proposed system is called µ-RCT-ACO-OFDM system. As a result of the results from the preceding section, we only employed RF values from 0.5 to 0.9 because they had superior performance in terms of PAPR and BER than values below 0.5.

4.2.1. a proposed system with RF=0.5 (SQRT Technique)

Figure. 5 explores PAPR performance when applying RCT to the proposed VLC system (i.e., Fig. 2). The figure also contains the performance of SQRT-ACO-OFDM and conventional ACO-OFDM (i.e., Fig. 1) for comparison purposes. In SQRT combined with A-law (A-SQRT), the companding factor (A) is set to vary by values 2, 3, 5, 7, and 10. At CCDF=10^{-3}, when A= 2, 3, 5, 7, and 10, the value of PAPR$_0$ equals 10.1, 9.5, 8.5, 8, and 7.1dB respectively. The reduction value for the different values of A-parameters equals 6.9, 7.5, 8.5, 9, and 9.9dB, respectively. In SQRT combined with µ-law (µ-SQRT), the companding factor (μ) is set to vary by values 2, 3, 5, 7, and 10. At CCDF=10^{-3}, when μ =2, 3, 5, 7, and 10, the value of PAPR$_0$ equals 9.1, 8.7, 8.3, 7.8, and 7.5dB respectively. The reduction value for the different values of μ -parameters equals 7.9, 8.3, 8.7, 9.2, and 9.5dB, respectively.
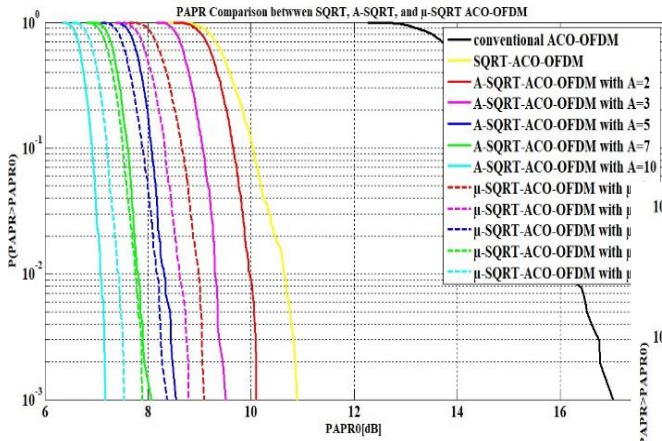
Fig. 5. PAPR Comparison between SQRT, A-SQRT, and μ-SQRT ACO-OFDM based VLC system with RF=0.5.

Figure. 6 shows that the BER performance of A-law and μ-law combined with SQRT. At BER=10^{-3}, the value of E_b/N_0 for conventional ACO-OFDM is equal to 13.5dB. For the companding factor A= 2 3, 5, 7, and 10, the required E_b/N_0 to achieve BER=10^{-3} are 14.6, 15, 16.9, 18.5 and 21dB, respectively. Thus, increased values in E_b/N_0 compared to conventional ACO-OFDM by 1.1, 1.5, 3.4, 5 and 7.5dB, respectively.
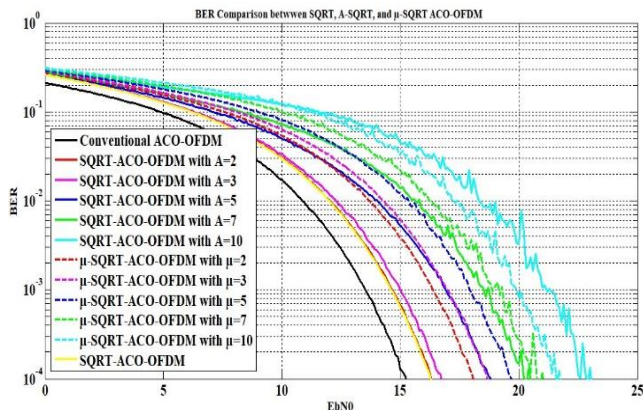
Fig. 6. BER Comparison between SQRT, A-SQRT, and μ-SQR -OFDM-based VLC system with RF=0.5.

4.2.2. Proposed system with RF=0.6, 0.7, 0.8, and 0.9.

The first analysis is carried out to determine the performance of the RCT when combined with A- and -law companding techniques. PAPR performance is shown in Figs. 7 into 8 for RF equals 0.6, 0.7, 0.8 and 0.9, respectively. In RCT combined with A-law companding techniques (A-RCT) and RCT combined with μ-law (μ-RCT), the value of PAPR reduction is increased by decreasing the RF parameter. The figures have shown the μ-RCT is effective in

PAPR reduction with a small value of companding (i.e., μ≤5). In A-RCT, The value of PAPR reduction with high companding factor A (i.e., A>5) is more effective compared to μ-RCT.
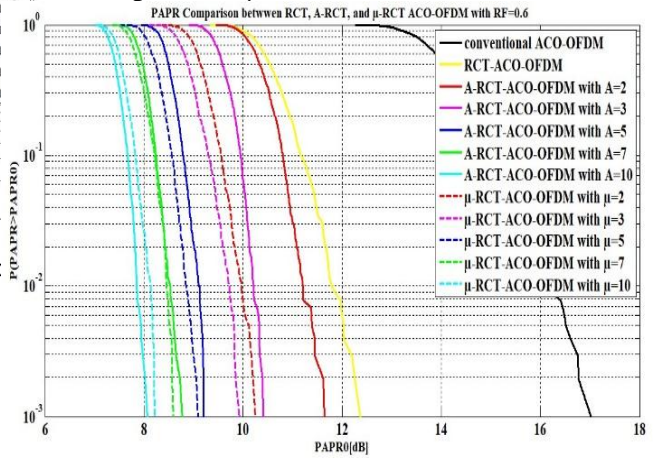
Fig. 7. PAPR Comparison between RCT, A-RCT, and μ-RCT ACO-OFDM with RF=0.6.
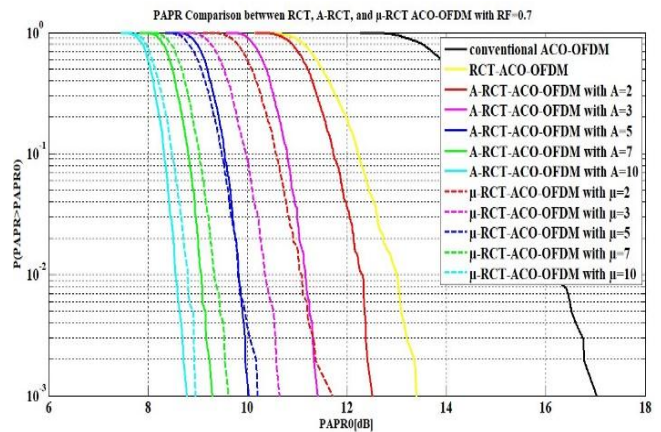
Fig. 8. PAPR Comparison between RCT, A-RCT, and μ-RCT ACO-OFDM with RF=0.7.
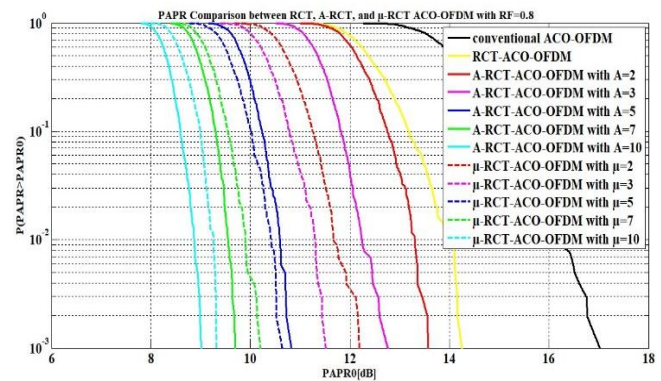
Fig. 9. PAPR Comparison between RCT, A-RCT, and μ-RCT ACO-OFDM with RF=0.8.

Fig. 10. PAPR Comparison between RCT, A-RCT, and μ-RCT ACO-OFDM RF=0.9.
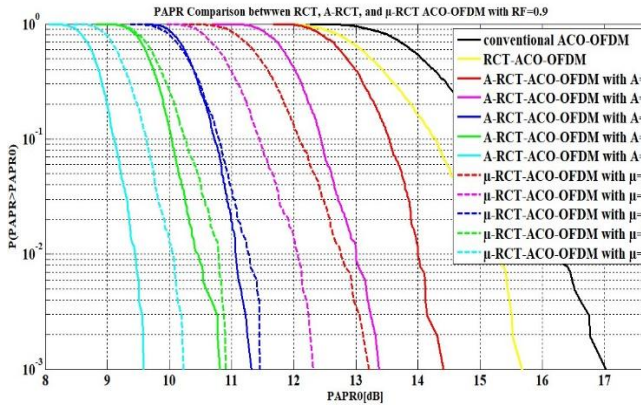
Fig. 11. BER Comparison between RCT, A-RCT, and μ-RCT ACO-OFDM with RF=0.6.

In conclusion, for all values of RF, for the low value of the companding factor, the μ- is better than A-law combined with RCT. However, for PAPR reduction, the proposed system's A-law companding techniques are more successful when A and μ factors are above 5.

Figure. 11 shows that the BER performance of a proposed system with RF=0.6. At BER=10^{-3}, the value of E_b/N_0 for conventional ACO-OFDM is equal to 13.5dB. For the companding factor, A equals 2 and 3, and the A-RCT shows a close behavior. For A equals 5, 7, and 10, the required E_b/N_0 to achieve BER=10^{-3} are 15.4, 16.8, and 18.6dB, respectively. Thus, increased values in E_b/N_0 compared to conventional ACO-OFDM by 1.9, 3.3, and 5.1dB, respectively. In μ-RCT, the companding factor μ equals 2, 3, 5, 7, and 10, the required E_b/N_0 to achieve BER=10^{-3} are 14.7, 15.1, 16.6, 17.3 and 18.3dB, respectively. Thus, increased values in E_b/N_0 compared to conventional ACO-OFDM by 1.2, 1.6, 3.1, 3.8, and 4.8dB, respectively.
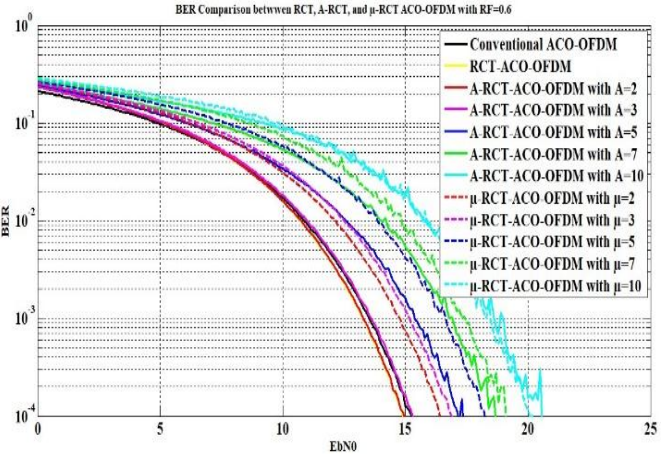
Starting from this section, the detailed data and discussion previously presented will be abbreviated greatly depending on Table 1 in section 4.3 and the following figures to avoid duplication and repetition. Only judgment on performance and evaluation for differences between merged techniques will be addressed.

Figures. 12 into 14 and data extracted from Table 1 lead to the observation that the BER performance for A-RCT and μ-RCT are quite similar at low companding factor (i.e., A and μ from 2 to 5) with attractive characteristics. μ-law at higher companding factors with RCT overcomes the performance A-law combined with the RCT. Finally, μ-law combined with WHT can be considered the optimum solution for the BER performance and power requirement.
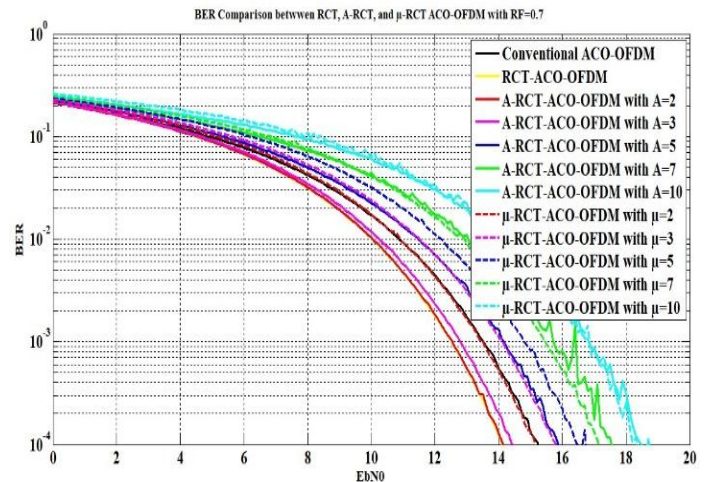
Fig. 12. BER Comparison between RCT, A-RCT, and μ-RCT ACO-OFDM with RF=0.7.
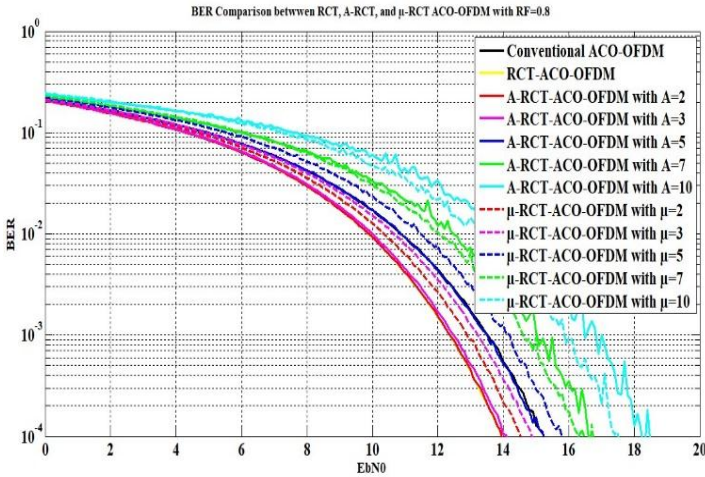
Fig. 13. BER Comparison between RCT, A-RCT, and μ-RCT ACO-OFDM with RF=0.8.
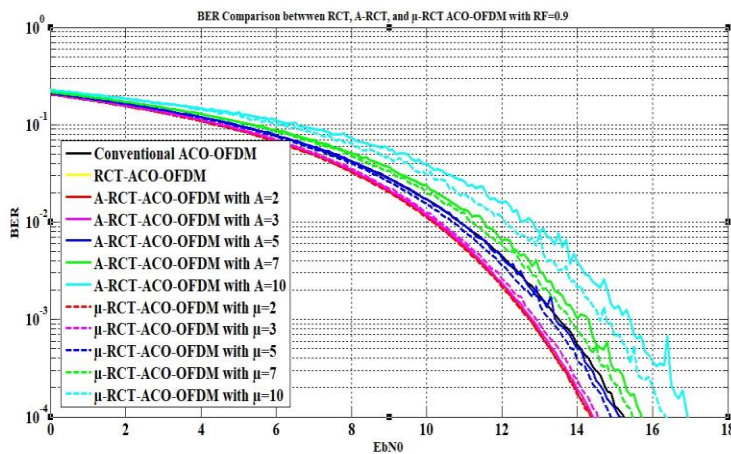
Fig. 14. BER Comparison between RCT, A-RCT, and μ-RCT ACO-OFDM with RF=0.9

4.3. Comparison between the RCT, A-RCT, and μ-RCT

In this section, a numerical comparison between RCT, A-RCT, and μ-RCT extracted from Figures 3 to 14 is carried out in Table 1. Similar to previous parameters and for comparing purposes, the values of $PAPR_0$ and E_b/N_0 are extracted at CCDF=10^{-3} and BER=10^{-3} respectively, where $PAPR_0$=17dB, E_b/N_0=13.5dB for conventional ACO-OFDM. PAPR reduction value and required ($E_b/N_{0\ diff}$) are used as evaluating parameters and are carried out in Table 1. Because PAPR is the primary focus of this work, the discussion that follows will focus exclusively on the performance of the merging techniques.

- For the merging between A-law companding with RCT, it is observed that:
1. The optimal PAPR performance is ranked by the rooting factor (RF), starting from 0.5 to 0.9 for all companding factors (A).

2. A high value of A is more effective in the value of PAPR reduction rather than the small value of A.

3. For BER performance, rooting factor 0.9 and 0.8, and companding factors from 2-5, the performance is better than the conventional ACO-OFDM.
4. For BER performance and compression factors greater than 7, the order of optimal performance is RF equals 0.9, then 0.8, and finally 0.5.

- For the merging between μ-law companding with RCT, it is observed that:
1. The optimal PAPR performance is RF=0.5, then 0.6, then 0.7, then 0.8, and finally 0.9.

For BER performance and companding factors ≤ 5 and RF=0.9 and 0.8, the performance-enhanced compared to conventional ACO-OFDM. ٠.٧ The performance of merging with .is close ٠.٥ ≥ FR ≥

The BER performance dropped significantly in comparison to conventional ACO-OFDM when the companding factors were above 5. The optimum BER performance in this range of companding factors is obtained through merging μ-law companding with RCT (i.e., RF=0.9 and 0.8).

- :ionAs conclus
1. When targeting a very high PAPR reduction value regarding BER performance (i.e., lousy BER performance), one can use RCT with a low RF value (i.e., RF<0.5).
2. A-RCT can provide an acceptable PAPR reduction value and reasonable BER performance when companding fator A is less than 7.
3. μ-RCT can only provide an acceptable PAPR reduction value and reasonable BER performance when companding fator μ is greater than or equal to 7.

5. Comparison with Related Studies

This section provides a detailed comparison of this work and related literature, as presented in Table 2. The key judgment factors definition and an indication of their values are those set with details at the beginning of section 4.

As shown in Table 2, this work has the unique advantage of achieving the highest calculated PAPR reduction value, which has

been set as the primary goal for all PAPR reduction-related literature. This is accomplished by selecting RCT combined with A-law companding techniques from among those discussed in this work. This result is associated with a large IFFT size (i.e., extensive data processing) and an acceptable modulation order. On the other hand, when the second lower priority judgment factor is considered ($E_b/N_{0\ diff}$), Table 2 indicates that for RCT combined with A-law companding techniques a 1.9 dB more power over E_b/N_0 for conventional ACO-OFDM (i.e., 13.5dB) is required to achieve the targeted BER (i.e., $=10^{-3}$). This is not a significant (i.e., less than zero is excellent) value; remarkable values for this factor can be found in Section 4.3, but at the cost of reduced PAPR and using other techniques rather than RCT combined with A-law companding techniques. Nonetheless, this value is more than acceptable, particularly the system's complexity achieved PAPR reduction value.

Table 1. $PAPR_0$ and E_b/N_0 Values at CCDF=10^{-3} & BER=10^{-3}. PAPR Reduction value and required Eb/N0 to achieve the same BER w.r.t Conventional ACO-OFDM, where $PAPR_0$=17dB, E_b/N_0 =13.5dB for ACO-OFDM

Companding Techniques	Companding factor	Root Companding Techniques (RCT), A-RCT, μ-RCT with ACO-OFDM			
		PAPR$_0$	PAPR reduction	E$_b$/N$_0$	E$_b$/N$_{0\ diff}$
RCT	0.1	4.9	12.1	29.8	16.3
	0.2	6.6	10.4	23.2	9.7
	0.3	8.1	8.9	19.3	5.8
	0.4	9.7	7.3	16.5	3
	0.5 (SQRT)	10.9	6.1	14.6	1.1
	0.6	12.4	4.6	13.2	-0.3
	0.7	13.4	3.6	12.5	-1
	0.8	14.3	2.7	12.3	-1.2
	0.9	15.7	1.3	12.7	-0.8

RCT Companding Factor		0.9	0.8	0.7	0.6	0.5	0.9	0.8	0.7	0.6	0.5	0.9	0.8	0.7	0.6	0.5	0.9	0.8	0.7	0.6	0.5
A-Law	2	14.4	13.5	12.5	11.6	10.1	2.6	3.5	4.5	5.4	6.9	12.7	12.3	12.5	13.3	14.6	-0.8	-1.2	-1	-0.2	1.1
	3	13.4	12.7	11.4	10.4	9.5	3.6	4.3	5.6	6.6	7.5	12.8	12.4	12.8	13.6	15	-0.7	-1.1	-0.7	0.1	1.5
	5	11.3	10.8	10	9.2	8.5	5.7	6.2	7	7.8	8.5	13.4	13.5	14.1	15.4	16.9	-0.1	0	0.6	1.9	3.4
	7	10.8	9.6	9.3	8.7	8	6.2	7.4	7.7	8.3	9	14	15	15.7	16.8	18.5	0.5	1.5	2.2	3.3	5
	10	9.6	9	8.8	8.1	7.1	7.4	8	8.2	8.9	9.9	15.3	16.5	16.8	18.6	21	1.8	3	3.3	5.1	7.5
μ-Law	2	13.2	12.2	11.3	10.2	9.1	3.8	4.8	5.7	6.8	7.9	12.7	12.8	13.4	14.7	16.3	-0.8	-0.7	-0.1	1.2	2.8
	3	12.3	11.5	10.6	9.9	8.7	4.7	5.5	6.4	7.1	8.3	12.9	13.2	14.1	15.1	16.9	-0.6	-0.3	0.6	1.6	3.4
	5	11.4	10.6	10.2	9.1	8.3	5.6	6.4	6.8	7.9	8.7	13.2	14.1	14.8	16.6	17.9	-0.3	0.6	1.3	3.1	4.4
	7	10.9	10.2	9.6	8.6	7.8	6.1	6.8	7.4	8.4	9.2	13.8	14.6	15.4	17.3	18.9	0.3	1.1	1.9	3.8	5.4
	10	10.2	9.3	8.9	8.2	7.5	6.8	7.7	8.1	8.8	9.5	14.6	15.8	16.8	18.3	19.9	1.1	2.3	3.3	4.8	6.4

Table 2.
A comparison between the studies and the presented work for different
PAPR Reduction techniques with ACO-OFDM

Ref	System	IFFT Size	Modulation Order	PAPR Reduction Value	$E_b/N_{0\ diff}$
[49]	Clipped ACO-OFDM with clipping mitigation using (TDCSR/FDCDR) [1]	1024	16-QAM	(5.6 dB / 5.3 dB)	acceptable
[50]	SACO-OFDM/ESACO-OFDM [2]	128	16-QAM 64-QAM 256-QAM	~ (1.2dB / 1.4dB)	1 dB 2 dB 3 dB
[51]	SVT-SLM [3]	512	16-QAM	~ 4.1 dB	NA
[52]	PA-OOFDM [4]	1024	M-QAM	~ 2.2 dB	NA
[53]	WHT-OOFDM DCT-OOFDM DHT-OOFDM VLM-OOFDM	256	16-QAM	0.93dB 1.89 dB 1.27 dB 2.9 dB	NA
[54]	RoC-ACO-OFDM [5] With MAP [6] - based detection algorithm	256	64-QAM	7.3dB	4dB
[55]	the Toeplitz matrix-based Gaussian blur method	256	16-QAM	6dB	~2dB
Proposed	RCT	1024	16-QAM	6.1dB	1.1dB
	A-RCT			7.8dB	1.9dB
	μ-RCT			7.7	2.3dB

[1]TDCSR/FDCDR=Time-Domain Clipped Sample Reconstruction/ Frequency – Domain Clipping Distortion Removal. [2]SACO-OFDM/ ESACO-OFDM= Subcarrier-index modulation-based ACO-OFDM/Enhanced SACO-OFDM. [3]SVT-SLM =Symmetric Vector Transformation- Selected Mapping. [4]PA-OOFDM=Pilot-Assisted Optical OFDM. [5]RoC-ACO-OFDM = Recoverable upper Clipping-ACO-OFDM. [6]MAP= Maximum A Posteriori.

6. CONCLUSION

This paper proposes many different PAPR reduction schemes for ACO-OFDM VLC systems. Tested and compared to one another, the proposed techniques are evaluated to identify an effective scheme capable of reducing PAPR to the greatest

extent possible while maintaining acceptable BER performance. The compatibility of ACO-OFDM schemes with practical applications is improved as a result of this research. The proposed μ-law companding technique combined with RCT archives the best performance possible at companding factors ranging from 2 to 10. For instance, a specified performance is obtained at RF=0.5 (SQRT technique) with a PAPR reduction of 6.1 dB and the $E_b/N_{0\ diff}$= 1.1 dB and a nominated performance is achieved at μ=10 and RF=0.8 with a PAPR reduction value equal to 7.7 dB and the $E_b/N_{0\ diff}$= 2.3 dB, and a nominated performance is achieved at A=5 and RF=0.6 with a PAPR reduction value equal to 7.8 dB and the $E_b/N_{0\ diff}$= 1.9 dB. A comparison with related litterateurs is carried out to validate and ensure the novelty of the proposed schemes with their performance.

REFERENCES

[1] N.A. Mohammed, M.A. Elkarim, Exploring the effect of diffuse reflection on indoor localization systems based on RSSI-VLC, Opt. Express. 23 (2015) 20297. https://doi.org/10.1364/oe.23.020297.

[2] L.E.M. Matheus, A.B. Vieira, L.F.M. Vieira, M.A.M. Vieira, O. Gnawali, Visible Light Communication: Concepts, Applications and Challenges, IEEE Commun. Surv. Tutorials. (2019). https://doi.org/10.1109/COMST.2019.2913348.

[3] N. a Mohammed, M.R. Abaza, M.H. Aly, Improved Performance of M-ary PPM in Different Free-Space Optical Channels due to Reed Solomon Code Using APD, 2 (2011) 2–5.

[4] N.A. Mohammed, A.H. Mansi, Performance enhancement and capacity enlargement for a DWDM-PON system utilizing an optimized cross seeding rayleigh backscattering design, Appl. Sci. 9 (2019). https://doi.org/10.3390/app9214520.

[5] N.A. Mohammed, H.O. El Serafy, Ultra-

sensitive quasi-distributed temperature sensor based on an apodized fiber Bragg grating, Appl. Opt. 57 (2018) 273. https://doi.org/10.1364/ao.57.000273.

[6] N.A. Mohammed, N.M. Okasha, Single- and dual-band dispersion compensation unit using apodized chirped fiber Bragg grating, J. Comput. Electron. 17 (2018) 349–360. https://doi.org/10.1007/s10825-017-1096-2.

[7] N. Mohammed, H. Abo, M. Aly, O. Member, Performance Evaluation and Enhancement of 2×2 Ti: LiNbO 3 Mach Zehnder Interferometer Switch at 1.3 μm and 1.55 μm, Perform. Eval. FSO Link Under NRZ-RZ Line Codes, Differ. Weather Cond. Receiv. Types Presence Pointing Errors. 6 (2012) 36–49.

[8] N.A. Mohammed, H.S. Abo Elnasr, M.H. Aly, Analysis and design of an electro-optic 2 × 2 switch using Ti: KNbO3 as a waveguide based on MZI at 1.3 μ m, Opt. Quantum Electron. 46 (2014) 295–304. https://doi.org/10.1007/s11082-013-9760-7.

[9] N.A. Mohammed, M.M. Hamed, A.A.M. Khalaf, S. EL-Rabaie, Malaria biosensors with ultra-sensitivity and quality factor based on cavity photonic crystal designs, Eur. Phys. J. Plus. 135 (2020). https://doi.org/10.1140/epjp/s13360-020-00940-5.

[10] N.A. Mohammed, M.M. Hamed, A.A.M. Khalaf, A. Alsayyari, S. El-Rabaie, High-sensitivity ultra-quality factor and remarkable compact blood components biomedical sensor based on nanocavity coupled photonic crystal, Results Phys. 14 (2019) 102478. https://doi.org/10.1016/j.rinp.2019.102478.

[11] T.S. Mostafa, N.A. Mohammed, E.S.M. El-Rabaie, Ultra-High bit rate all-optical AND/OR logic gates based on photonic crystal with multi-wavelength simultaneous operation, J. Mod. Opt. 66 (2019) 1005–1016. https://doi.org/10.1080/09500340.2019.1598587.

[12] T.S. Mostafa, N.A. Mohammed, E.S.M. El-Rabaie, Ultracompact ultrafast-switching-speed all-optical 4 × 2 encoder based on photonic crystal, J. Comput. Electron. 18 (2019) 279–292. https://doi.org/10.1007/s10825-018-1278-6.

[13] A. Jovicic, J. Li, T. Richardson, Visible light communication: opportunities, challenges and the path to market, IEEE Commun. Mag. 51 (2013) 26–32.

[14] S.U. Rehman, S. Ullah, P.H.J. Chong, S. Yongchareon, D. Komosny, Visible light communication: A system perspective—Overview and challenges, Sensors (Switzerland). 19 (2019). https://doi.org/10.3390/s19051153.

[15] I.C. Rust, H.H. Asada, A dual-use visible light approach to integrated communication and localization of underwater robots with application to non-destructive nuclear reactor inspection, Proc. - IEEE Int. Conf. Robot. Autom. (2012) 2445–2450. https://doi.org/10.1109/ICRA.2012.6224718.

[16] N.A. Mohammed, K.A. Badawi, A.A.M. Khalaf, S. El-Rabaie, Dimming control schemes combining IEEE 802.15.7 and SC-LPPM modulation schemes with an adaptive M-QAM OFDM for indoor LOS VLC systems, Opto-Electronics Rev. 28 (2020) 203–212. https://doi.org/10.24425/opelre.2020.135259.

[17] N.A. Mohammed, K.A. Badawi, Design and Performance Evaluation for a Non-Line of Sight VLC Dimmable System Based on SC-LPPM, IEEE Access. 6 (2018) 52393–52405. https://doi.org/10.1109/ACCESS.2018.2869878.

[18] M.H. Shoreh, A. Fallahpour, J.A. Salehi, Design concepts and performance analysis of multicarrier CDMA for indoor visible light communications, J. Opt. Commun. Netw. (2015). https://doi.org/10.1364/JOCN.7.000554.

[19] M.S.A. Mossaad, S. Hranilovic, L. Lampe, Visible Light Communications Using OFDM and Multiple LEDs, IEEE Trans. Commun. (2015). https://doi.org/10.1109/TCOMM.2015.2469285.

[20] K.A. Badawi, N.A. Mohammed, M.H. Aly, Exploring BER performance of a SC-LPPM based LOS-VLC system with distinctive lighting, J. Optoelectron. Adv. Mater. 20 (2018) 290–301.

[21] N.A. Mohammed, M.M. Elnabawy, A.A.M. Khalaf, Opto-Electronics Review PAPR reduction using a combination between precoding and non-linear companding techniques for ACO-OFDM-based VLC systems, 29 (2021) 59–70. https://journals.pan.pl/dlibra/publication/135829/edition/118752/content.

[22] D. Tsonev, S. Sinanovic, H. Haas, Novel unipolar orthogonal frequency division multiplexing (U-OFDM) for optical wireless, IEEE Veh. Technol. Conf. (2012). https://doi.org/10.1109/VETECS.2012.6240060.

[23] W.W. Hu, PAPR Reduction in DCO-OFDM Visible Light Communication Systems Using Optimized Odd and even Sequences Combination, IEEE Photonics J. 11 (2019) 1–15. https://doi.org/10.1109/JPHOT.2019.2892871.

[24] J. Dang, Z. Zhang, L. Wu, Improving the power efficiency of enhanced unipolar OFDM for optical wireless communication, Electron. Lett. 51 (2015) 1681–1683. https://doi.org/10.1049/el.2015.2024.

[25] A.J. Lowery, Comparisons of spectrally-enhanced asymmetrically-clipped optical OFDM systems, Opt. Express. 24 (2016) 3950. https://doi.org/10.1364/oe.24.003950.

[26] T. Zhang, J. Zhou, Z. Zhang, Y. Qiao, F. Su, A. Yang, A performance improvement and cost-efficient ACO-OFDM scheme for visible light communications, Opt. Commun. 402 (2017) 199–205. https://doi.org/10.1016/j.optcom.2017.06.015.

[27] E. Shawky, M.A. El-Shimy, H.M.H. Shalaby, A. Mokhtar, E.-S.A. El-Badawy, Kalman Filtering for VLC Channel Estimation of ACO-OFDM Systems, in: 2018 ASIA Commun. PHOTONICS Conf., IEEE, 345 E 47TH ST, NEW YORK, NY 10017 USA, 2018.

[28] S. Vappangi, V.M. Vakamulla, Channel estimation in ACO-OFDM employing different transforms for VLC, AEU - Int. J. Electron. Commun. 84 (2018) 111–122. https://doi.org/10.1016/j.aeue.2017.11.016.

[29] M.M. Hasan, VLM precoded SLM technique for PAPR reduction in OFDM systems, Wirel. Pers. Commun. 73 (2013) 791–801. https://doi.org/10.1007/s11277-013-1217-6.

[30] M.Z. Afgani, H. Haas, H. Elgala, D. Knipp, Visible light communication using OFDM, in: 2nd Int. Conf. Testbeds Res. Infrastructures Dev. Networks Communities, TRIDENTCOM 2006, 2006. https://doi.org/10.1109/TRIDNT.2006.1649137.

[31] M.A. Elkarim, M.H. Aly, H.M. AbdelKader, M.M. Elsherbini, LED nonlinearity mitigation in LACO-OFDM optical communications based on adaptive predistortion and postdistortion techniques, Appl. Opt. 60 (2021) 7279–7289. https://doi.org/10.1364/AO.432364.

[32] M.A. Elkarim, M.M. Elsherbini, H.M. AbdelKader, M.H. Aly, Exploring the effect of LED nonlinearity on the performance of layered ACO-OFDM, Appl. Opt. 59 (2020) 7343–7351. https://doi.org/10.1364/AO.397559.

[33] M. Mounir, I.F. Tarrad, M.I. Youssef, Performance evaluation of different precoding matrices for PAPR reduction in OFDM systems, Internet Technol. Lett. 1 (2018) e70. https://doi.org/10.1002/itl2.70.

[34] M.M. Hasan, VLM precoded SLM technique for PAPR reduction in OFDM systems, Wirel. Pers. Commun. 73 (2013) 791–801. https://doi.org/10.1007/s11277-

013-1217-6.

[35] H. Freag, et al., PAPR Reduction in VLC-OFDM System using CPM Combined with PTS Method, Int. J. Comput. Digit. Syst. 6 (2017) 127–132. https://doi.org/10.12785/ijcds/060304.

[36] Y. Xiao, M. Chen, F. Li, J. Tang, Y. Liu, L. Chen, PAPR reduction based on chaos combined with SLM technique in optical OFDM IM/DD system, Opt. Fiber Technol. 21 (2015) 81–86. https://doi.org/10.1016/j.yofte.2014.08.0 14.

[37] S. Hu, G. Wu, Q. Wen, Y. Xiao, S. Li, Nonlinearity reduction by tone reservation with null subcarriers for WiMAX system, Wirel. Pers. Commun. 54 (2010) 289–305. https://doi.org/10.1007/s11277-009-9726-z.

[38] X. Zhang, Q. Wang, R. Zhang, S. Chen, L. Hanzo, Performance Analysis of Layered ACO-OFDM, IEEE Access. 5 (2017) 18366–18381. https://doi.org/10.1109/ACCESS.2017.2 748057.

[39] K. Anoh, C. Tanriover, B. Adebisi, M. Hammoudeh, A New Approach to Iterative Clipping and Filtering PAPR Reduction Scheme for OFDM Systems, IEEE Access. 6 (2017) 17533–17544. https://doi.org/10.1109/ACCESS.2017.2 751620.

[40] D. Madhavi, M. Ramesh Patnaik, Implementation of Non Linear Companding Technique for Reducing PAPR of OFDM, Mater. Today Proc. 5 (2018) 870–877. https://doi.org/10.1016/j.matpr.2017.11. 159.

[41] I.A.A. Shaheen, A. Zekry, F. Newagy, R. Ibrahim, Absolute Exponential Companding to Reduced PAPR for FBMC/OQAM, Proc. - 2017 Palest. Int. Conf. Inf. Commun. Technol. PICICT 2017. (2017) 60–65. https://doi.org/10.1109/PICICT.2017.17.

[42] Y. Yang, Z. Zeng, S. Feng, C. Guo, A Simple OFDM Scheme for VLC Systems Based on μ-Law Mapping, IEEE Photonics Technol. Lett. 28 (2016) 641–644. https://doi.org/10.1109/LPT.2015.2503481.

[43] A.K. Yadav, Y.K. Prajapati, PAPR Minimization of Clipped OFDM Signals Using Tangent Rooting Companding Technique, Wirel. Pers. Commun. 105 (2019) 1435–1447. https://doi.org/10.1007/s11277-019-06151-1.

[44] Z. Ghassemlooy, C. Ma, S. Guo, PAPR reduction scheme for ACO-OFDM based visible light communication systems, Opt. Commun. 383 (2017) 75–80.

[45] M. Abd Elkarim, M.M. Elsherbini, H.M. AbdelKader, M.H. Aly, Exploring the effect of LED nonlinearity on the performance of layered ACO-OFDM, Appl. Opt. 59 (2020) 7343–7351. https://doi.org/10.1364/AO.397559.

[46] V. Kumar Singh, U.D. Dalal, Abatement of PAPR for ACO-OFDM deployed in VLC systems by frequency modulation of the baseband signal forming a constant envelope, Opt. Commun. 393 (2017) 258–266. https://doi.org/10.1016/j.optcom.2017.02.0 65.

[47] M.M. El-Nabawy, M.A. Aboul-Dahab, K. El-Barbary, PAPR Reduction of OFDM Signal By Using Combined Hadamard and Modified Meu-law Companding Techniques, Int. J. Comput. Networks Commun. 6 (2014) 71.

[48] Y.S. Reddy, M.V.K. Reddy, K. Ayyanna, G. V Ravikumar, The Effect of NCT Techniques on SC-FDMA System in presence of HPA, 3 (2014) 844–848.

[49] A.F. Abd El-Rahman, R.A. Ahmed, M.M. Abd Elnaby, S. Khamis, S. Napoleon, M. Abd-Elnaby, Z.A. Ahmed, E.S.M. El-Rabaie, F.E. Abd El-Samie, Companding techniques for SC-FDMA and sensor network applications, Int. J. Electron. Lett. 8 (2020) 241–255. https://doi.org/10.1080/21681724.2019.160 0051.

[50] A.W. Azim, Y. Le Guennec, G. Maury,

Decision-directed iterative methods for PAPR reduction in optical wireless OFDM systems, Opt. Commun. 389 (2017) 318–330. https://doi.org/10.1016/j.optcom.2016.12.026.

[51] R. Guan, W. Xu, Z. Yang, N. Huang, J.Y. Wang, M. Chen, Enhanced subcarrier-index modulation-based asymmetrically clipped optical OFDM using even subcarriers, Opt. Commun. 402 (2017) 600–605. https://doi.org/10.1016/j.optcom.2017.06.032.

[52] W.W. Hu, SLM-based ACO-OFDM VLC system with low-complexity minimum amplitude difference decoder, Electron. Lett. 54 (2018) 144–146. https://doi.org/10.1049/el.2017.3158.

[53] Z. Wang, Z. Wang, S. Chen, Encrypted image transmission in OFDM-based VLC systems using symbol scrambling and chaotic DFT precoding, Opt. Commun. 431 (2019) 229–237. https://doi.org/10.1016/j.optcom.2018.09.045.

[54] F.B. Offiong, S. Sinanovic, W.O. Popoola, On PAPR Reduction in Pilot-Assisted Optical OFDM Communication Systems, IEEE Access. 5 (2017) 8916–8929. https://doi.org/10.1109/ACCESS.2017.2700877.

[55] W. Xu, M. Wu, H. Zhang, X. You, C. Zhao, ACO-OFDM-specified recoverable upper clipping with efficient detection for optical wireless communications, IEEE Photonics J. 6 (2014). https://doi.org/10.1109/JPHOT.2014.2352643.